

# Phenomenological model for a novel melt-freeze phase of sliding bilayers

Trieu Mai

Department of Physics, University of California, Santa Cruz, CA 95064.

(Dated: April 10, 2017)

Simulations show that sliding bilayers of colloidal particles can exhibit a new phase, the “melt-freeze” phase, where the layers stochastically alternate between solidlike and liquidlike states. We introduce a mean field phenomenological model with two order parameters to understand the interplay of two adjacent layers while the system is in this remarkable phase. Predictions from our numerical simulations of a system in the melt-freeze phase include the tendency of two adjacent layers to be in opposite states (solid and liquid) and the difference between the fluctuation of the order parameter in one layer while the other layer is in the same phase compared to the fluctuation while the other layer is in the opposite phase. We expect this behavior to be seen in future simulations and experiments.

PACS numbers:

## I. INTRODUCTION

General theories of nonequilibrium phenomena are still elusive and current research in nonequilibrium physics is directed on a phenomenon-by-phenomenon basis. One important problem is the shear-induced melting (and/or freezing) of a solid. The shear flow of a solid is widely studied experimentally [1] due to its importance in material science. Being a standard example of the rich field of nonequilibrium phase transitions, shear-induced melting is also widely studied theoretically on systems as diverse as vortex lattices to suspended colloidal particles [1, 2, 3, 4].

For clarity, we will focus on a specific system of colloidal particles on two dimensional sheets [2]. An isolated sheet at low enough temperature will have colloidal particles in an ordered phase. When two such sheets are driven across each other, one sheet subjects stress on the other (and vice versa) and at high enough stresses, could induce melting [4]. At large enough driving forces, the sheets are occasionally found to re-order to a re-entrant solid phase displaying, the phenomenon of shear-induced freezing [5].

Recently, numerical simulations of sliding bilayers by Das *et al.* [4, 6] discovered a new “melt-freeze” phase beyond the standard shear-induced phases. Das *et al.* performed Brownian dynamics simulations of particles on two adjacent monolayers in the manner described in the previous paragraph. Earlier simulations usually contain one monolayer driven across a fixed substrate [4] which is applicable when one layer is much stiffer than the other. However the simulations of Das *et al.* addressed the situation in which two comparably soft layers are driven across each other and thus the behavior of the particles on *both* layers becomes important. The relevant parameters in their simulations included the strength of the driving force, the magnitude of the coupling between particles on differing sheets, and the noise amplitude. Changing these parameters displays rich and unexpected behavior.

Das *et al.* found that at fixed interlayer coupling and noise strength, the system undergoes different phases as

the driving force is varied. For small driving forces, the two monolayers remain in the ordered phase and simply creep past one other. The same qualitative behavior is seen for very large driving forces. However, at intermediate driving forces, the two monolayers undergo a melt-freeze phase in which both layers stochastically disorder (melt) and order (freeze). As the interlayer coupling increases, the melt-freeze phase persists over a larger range of driving forces. For a fixed driving force (in which the system is in the melt-freeze phase), increasing the coupling also increases the amount of time a layer spends in the disordered state.

In addition to the simulation of particles on layers, Das *et al.* introduced a simple mean field phenomenological model [4]. This phenomenological model contains one order parameter and a strain variable. Like the spatially dependent system, the mean field model has three simulation parameters (noise strength, coupling strength, and driving force). Remarkably, this simple model contains much of the rich behavior of the more detailed particle simulations. However, the interplay between the two layers cannot be studied by this model with only one order parameter. The simple model also clearly connects the melt-freeze phase with stochastic resonance phenomena [4, 7].

In this paper, we closely follow but extend the phenomenology in [4] to include two order parameters  $\rho_1$  and  $\rho_2$  in the same spirit that Das *et al.*’s particle simulations [4, 6] generalized the conventional models of one sheet sliding over a fixed substrate. This natural extension qualitatively recovers much of the behavior seen in the one order parameter phenomenological model (therefore also in the particle model). In addition, we observe two new features involving how one order parameter affects the free energy landscape of the other. The first feature is the tendency of the two order parameters to be in different phases when the coupling is finite, *i.e.* when  $\rho_1$  is in the ordered phase,  $\rho_2$  is likely to be in the disordered phase. The second feature involves the fluctuation of the order parameters. When  $\rho_1$  and  $\rho_2$  are out of phase, their fluctuations are smaller than when they are

in the same phase. These features are compared to the simulation of particles in [4, 6].

In the next section, we describe our two parameter Landau model and the Langevin-Ginzburg dynamics. Section III contains the results from our simulations. As in [4, 6], the results include driving force dependence and coupling strength dependence.

## II. MODEL FREE ENERGY AND DYNAMICS

The order parameter in our mean field model represents the structure factor for the colloidal particles in a given sheet [8]. The model free energy must represent a system with two phases (crystal and liquid) and contain a first order transition between the phases. A simple effective Landau free energy with these considerations is the simple double well potential used in Ref. [4, 6],

$$V(\rho) = \frac{\alpha}{2}\rho^2 - \frac{\beta}{3}\rho^3 + \frac{\gamma}{4}\rho^4, \quad (1)$$

where  $\alpha, \beta$ , and  $\gamma$  are all positive. The values are chosen so that there are two phases (two minima) and the stable phase is the crystalline one when there is no stress.

Modelling the dynamically driven phase transitions requires a strain variable  $\theta$ , as in [4, 6]. Since stress is induced by a periodic crystal, the strain variable must be periodic (we use the range  $[0, 1)$ ). A liquid does not induce stress on a driven solid sheet. Using these properties of strain, we model the part of the free energy with the strain variable to be [9]

$$W(\rho_1, \rho_2, \theta) = \frac{c}{2}\rho_1^2\rho_2^2[1 - \cos(2\pi\theta)], \quad (2)$$

where  $c$  is a coupling strength. The total model free energy includes both order parameters in a free energy landscape of Eq.(1) and the strain variable and coupling of Eq.(2),

$$F(\rho_1, \rho_2, \theta) = V(\rho_1) + V(\rho_2) + W(\rho_1, \rho_2, \theta). \quad (3)$$

Figure 1 shows the free energy for an order parameter while the other is in the ordered state. Since the other sheet is ordered, it can induce stress. As stress increases, shown by a larger  $\theta$ , the ordered phase becomes less stable and the system is driven towards the liquid phase. The changing landscape shown in figure 1 shows how the simple free energy of Eq.(3) can represent shear-induced melting.

Eq.(3) displays the equilibrium conditions in which the order parameters exist. For these driven systems, the dynamics are also important. In this paper, we use overdamped Langevin dynamics of the form

$$\begin{aligned} \dot{\rho}_1 &= -\frac{1}{\Gamma_\rho} \frac{\partial F}{\partial \rho_1} + \eta_\rho, \\ \dot{\rho}_2 &= -\frac{1}{\Gamma_\rho} \frac{\partial F}{\partial \rho_2} + \eta_\rho, \\ \dot{\theta} &= -\frac{1}{\Gamma_\theta} \frac{\partial F}{\partial \theta} + d + \eta_\theta. \end{aligned} \quad (4)$$

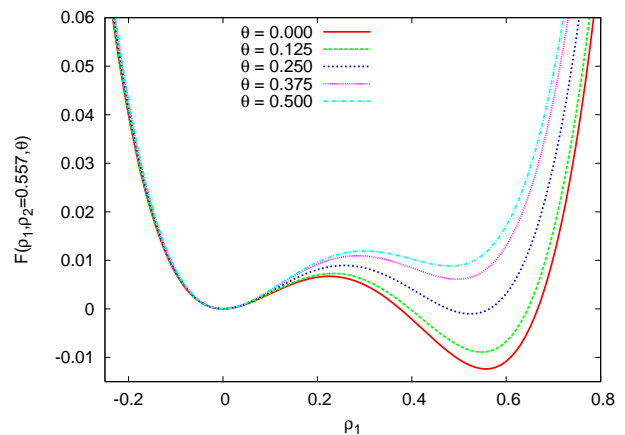


FIG. 1: The free energy for one order parameter  $\rho_1$  while the other order parameter  $\rho_2$  is in the ordered state. The different plots represent different values of  $\theta$  from 0.0 (no stress) to 0.5 (maximal stress). The coupling  $c$  is set to 0.25 here and  $\alpha = 1, \beta = 6.25$ , and  $\gamma = 8$ .

The damping coefficients  $\Gamma$ 's are set to unity,  $d$  represents a constant driving force for the strain, and the  $\eta$ 's represent noise. We use Gaussian noise with zero mean  $\langle \eta \rangle = 0$  and variance  $D$ ,  $\langle \eta(t)\eta(t') \rangle = 2D\delta(t - t')$ . The amount of noise  $D$  is related to the temperature through the fluctuation-dissipation theorem. The strain variable and the order parameters have noise of equal amplitudes in our simulations.

Eq.(3) and Eqs.(4) describe the free energy and dynamics of our phenomenological model. In the next section, we briefly describe the numerical implementation of these equations and the results of our simulations.

## III. RESULTS

We numerically integrate the Langevin-Ginzburg equations, Eqs.(4), using the fourth order Runge-Kutta algorithm. For all simulations, the stepsize is 0.001 and the integrator is run for  $\sim 10^6$  transient steps which are discarded. We also set  $\alpha = 1, \beta = 6.25$ , and  $\gamma = 8$  for all simulations. As in [4, 6], the adjustable parameters in the model are the strength of the constant driving force  $d$ , the coupling strength  $c$ , and the noise amplitude  $D$ . Below, we show how the system behaves by varying these parameters independently. To study the variation of the driving force and the coupling, we keep the noise amplitude fixed at  $D = 0.004$ . We observe that this noise strength is insufficient to drive the system to the disordered phase from the ordered phase for very long times when stress is absent.

### A. Driving Force Dependence

As described in the introduction and in [4, 6], the system stays essentially crystalline when the driving force is below a threshold value or above another threshold. Only at intermediate driving forces is the melt-freeze phase seen. In figure 2 we show  $\rho_1$  and  $\rho_2$  versus time at constant coupling,  $c = 0.25$ . The unit of time in figure 2 and figure 5 represents  $2 \times 10^4$  timesteps. Figure 3 shows the distribution of  $\rho_1$  (the distribution of  $\rho_2$  is the same after averaging over long enough time due to the symmetry between the two in the free energy).

To understand this behavior qualitatively, we discuss the role of the strain variable in determining the phase of the system. The driving force tilts the cosine potential and drives the strain variable in a preferred direction. At very small driving forces, the strain variable is rarely able to leave the minimum in which it started. As seen from figure 1, when  $\theta$  is near this minimum the crystal well remains stable and  $\rho$  does not cross the barrier. For very large driving forces the cosine potential is not seen and the distribution of  $\theta$  is essentially flat and does not spend enough time near its peak to allow  $\rho$  to cross over to the liquid well. In between these two limits exists an optimal value for  $d$ . Figure 4 shows the distribution of  $\theta$  (since  $\theta$  is periodic from zero to one, it is only necessary to display the distribution of the decimal) for different driving forces. As  $d$  increases, the peak in the distribution moves to a greater value and the whole distribution flattens.

From these figures, it is clear that there is an optimal driving force in which the melt-freeze phase exists. This behavior qualitatively agrees with both the particle simulations and the one order parameter phenomenological model in [4, 6].

### B. Coupling Dependence

Keeping the driving force at a fixed value of  $d = 0.1$  (which is near the optimal value), we observe the behavior of the system as the coupling constant varies. Figure 5 shows the order parameters versus time and figure 6 shows the distribution of  $\rho_1$  for different couplings.

Since the driving force is taken to be near the optimal value, all three cases from figures 5 and 6 are in the melt-freeze phase. From these figures, it is clear that as the coupling strength increases, the time spent in the liquid phase increases as well, which is a feature seen in the models of Das *et al.* Furthermore, systems with larger coupling strengths have order parameters that tend to be in opposite phases.

To explore this further, we define the boundary between the two phases to be the location of the local maximum without stress,  $\rho = (1/2\gamma)[\beta - (\beta^2 - 4\alpha\gamma)^{1/2}]$ , and calculate how often  $\rho_1$  and  $\rho_2$  are in the same well. In the weak coupling case ( $c = 0.2$ ), the two order parameters are in the same well approximately 80 percent of the

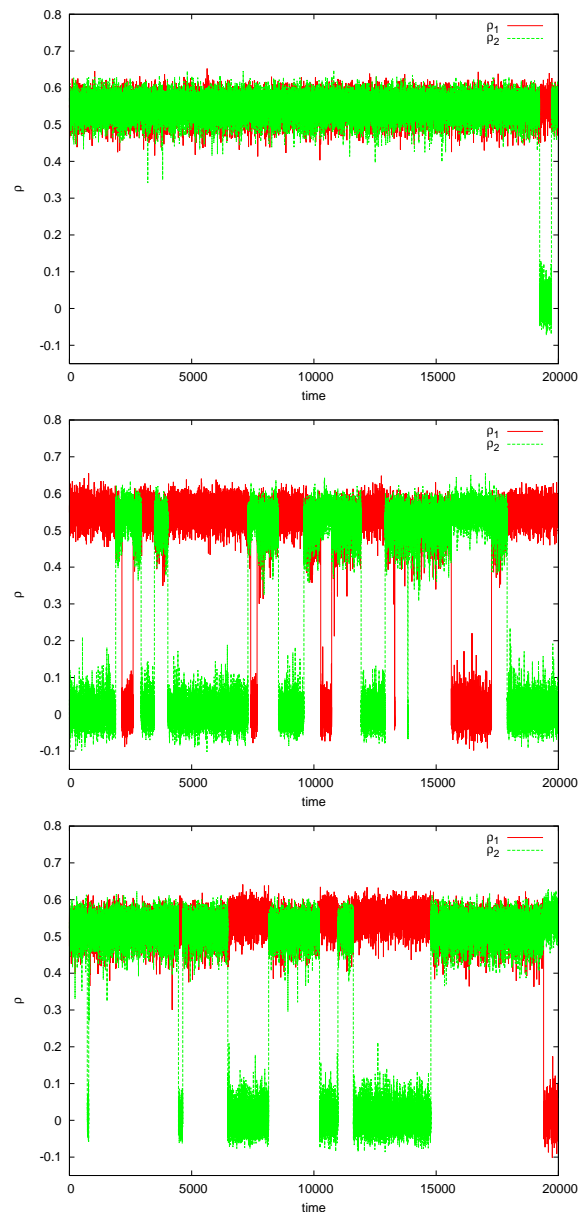


FIG. 2: The order parameter vs. time for three different driving forces  $d = 0.025, 0.1$ , and  $10.0$  respectively from top to bottom. The coupling  $c = 0.25$  and noise strength  $D = 0.004$  are kept fixed.

time. For the medium coupling case ( $c = 0.25$ ),  $\rho_1$  and  $\rho_2$  are in the same phase approximately 35 percent of the time and in the large coupling case ( $c = 0.3$ ), they only reside in the same well about 10 percent of the time. In the infinite coupling limit, the two order parameters will “repel” each other rather strongly. Due to the symmetry in the free energy between  $\rho_1$  and  $\rho_2$ , in this limit, each order parameter has the same probability of being in the ordered phase as the disordered.

The observation described in the above paragraph provides a new prediction for spatially dependent simula-

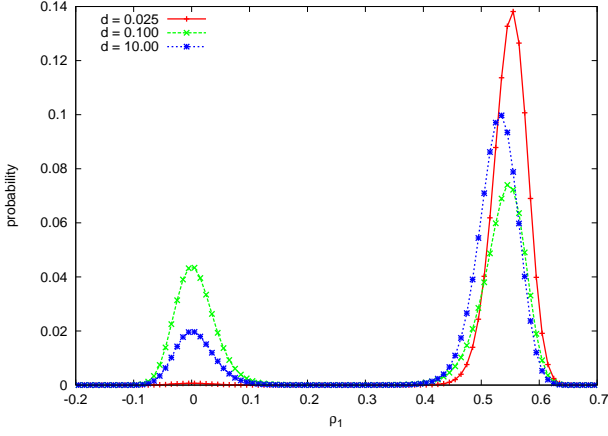


FIG. 3: The distribution of  $\rho_1$  taken over  $10^{11}$  steps for  $d = 0.025, 0.1$ , and  $10.0$ . The coupling  $c = 0.25$  and noise strength  $D = 0.004$  are kept fixed.

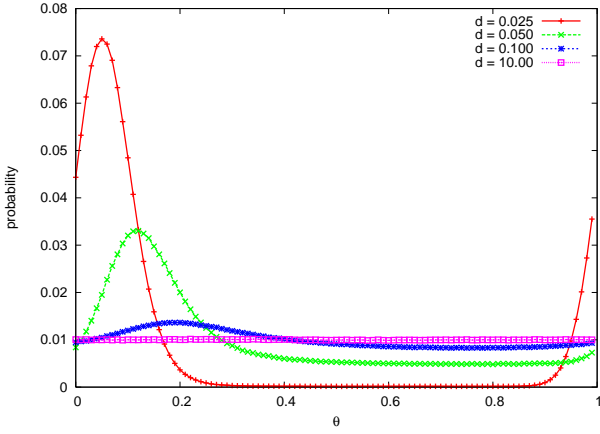


FIG. 4: The distribution of  $\theta$  taken over  $10^{11}$  steps for  $d = 0.025, 0.05, 0.1$ , and  $10.0$ . The coupling  $c = 0.25$  and noise strength  $D = 0.004$  are kept fixed.  $\theta$  is periodic in the range  $[0, 1)$ .

tions and experiments. Obviously, the behavior seen here cannot be seen in the one order parameter mean field model.

By observing that the coupling term in the free energy merely changes the coefficient of the quadratic term for a given order parameter, one can intuitively understand this behavior. In the large coupling regime, the landscape in which  $\rho_1$  exists is strongly determined by  $\rho_2$  and  $\theta$ . If both start in the crystal well, as soon as  $\theta$  is finite, this minimum quickly becomes unstable and one of the  $\rho$ 's must roll down to the disordered minimum. If  $\rho_2$  falls down the liquid well, the amplitude of the effective coupling drops near zero and  $\rho_1$  is again happily in its stable well. In addition, from  $\rho_2$ 's perspective, it is also in its own stable well because  $c\rho_1^2/2$  is finite and large. Since the height of the cosine potential is proportional to both

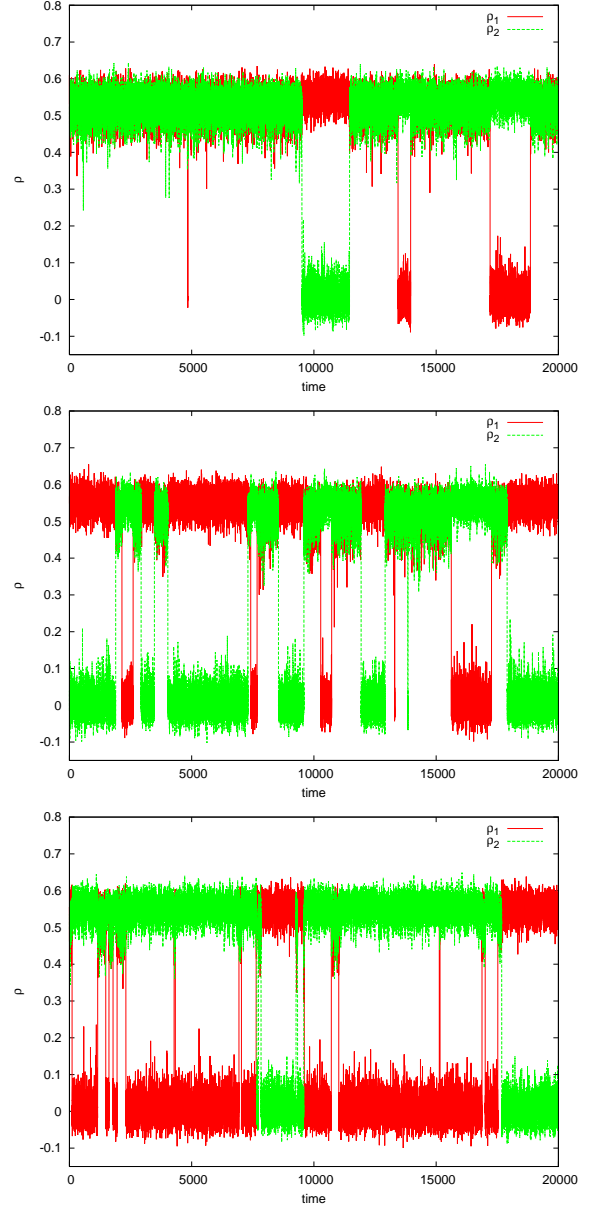


FIG. 5: The order parameter vs. time for three different coupling strengths  $c = 0.2, 0.25$ , and  $0.3$  respectively from top to bottom. The driving force  $d = 0.1$  and noise strength  $D = 0.004$  are kept fixed.

order parameters squared, when one order parameter is in the liquid phase,  $\theta$  is essentially driven without resistance. Driving the strain variable in this way allows the crystal well to become stable for  $\rho_2$ . With aid of noise,  $\rho_2$  can eventually move back to the crystal phase. But once this occurs, both order parameters are in a highly unstable position and one will quickly leave for the liquid phase and the situation repeats itself. Which one crosses to the liquid phase first is a stochastic process and cannot be determined, but the repulsion effect still remains.

The simulations of layers of particles in [4, 6] show

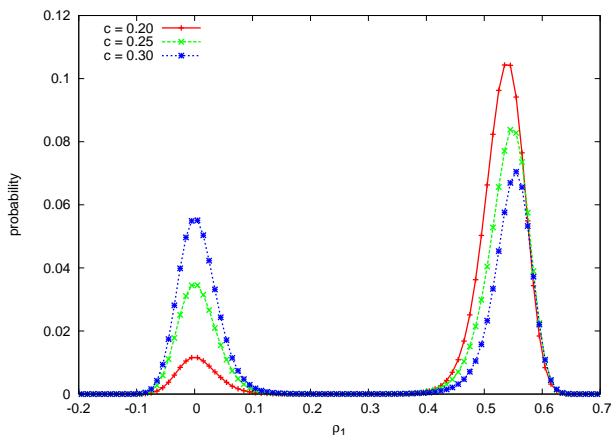


FIG. 6: The distribution of  $\rho_1$  taken over  $10^{11}$  steps for  $c = 0.2, 0.25$ , and  $0.3$ . The driving force  $d = 0.1$  and noise strength  $D = 0.004$  are kept fixed.

hints of this repulsive behavior though this repulsion is not as explicitly seen as in our mean field model. Our phenomenological model provides intuition into this behavior and predicts that it should be more easily seen as the coupling increases. More work is necessary to verify whether this is seen in a spatially dependent model.

With the form of our model free energy and the parameters in our simulations, the repulsive behavior is so strong that the system has yet to be seen in a state where both order parameters are in the disordered phase. Though this has not been seen in our simulations, the stochastic nature allows this state to be possible and, presumably, parameters can be tuned so that both order parameters can be in the liquid well in a quasi-stable state.

### C. Fluctuations

A close inspection of figures 2 and 5 reveals interesting behavior regarding the fluctuations of the order parameters; the fluctuation of one order parameter depends on the state of the other order parameter. Obviously, the noise amplitude and shape of the well determines the amount an order parameter fluctuates. The magnitude of the other order parameter (and the strain) influences the quadratic term of the free energy, thereby changing the shape of the well.

Figures 2 and 5 show that the fluctuations of an order parameter in the crystalline well is much larger when the other order parameter resides in the same well. To quantify this, we compare the standard deviation of  $\rho_1$  while both  $\rho_1$  and  $\rho_2$  are in the crystalline well ( $\rho > (1/2\gamma)[\beta - (\beta^2 - 4\alpha\gamma)^{1/2}]$ ) to the standard deviation while  $\rho_1$  is ordered and  $\rho_2$  is disordered. For  $c = 0.25, d = 0.1$ , and  $D = 0.004$ , the standard deviation is approximately 0.039 for the former and 0.028 for the latter.

This behavior makes physical sense because when both layers are solid, stress is induced between the two layers and the particles are driven further away from their equilibrium positions. Whereas, if the particles in one layer are disordered, the layer will not induce any stress on the neighboring layer.

## IV. DISCUSSION

We note two minor disagreements between our mean field model and the more detailed particle simulations of Das *et al.* [4, 6]. The first is that Das *et al.* observed a smaller extent of order with smaller interlayer coupling whereas we observe the opposite, *i.e.* for our model, the mean value for  $\rho$  in the crystalline state is larger for smaller coupling  $c$ . The second disagreement is that for larger coupling we see larger fluctuations of the order parameter while Das *et al.* observed a decrease in the amount of the fluctuations. Considering the simplicity of the phenomenological model, disparities such as these are expected and the many agreements are quite surprising.

By varying the noise in the one order parameter phenomenological model, Das *et al.* connects this melt-freeze phase to stochastic resonance [4]. Qualitatively, the optimal driving force exists when the driving time constant matches (within perhaps a factor of two) the thermal barrier crossing time constant. Conversely, with a fixed driving force, one expects a small window of noise amplitudes where the thermal escape rate “resonates” with the driving rate. The existence of an optimal noise amplitude [10] is a signature of stochastic resonance [7]. Due to the similarities of that model and ours, we expect that our model displays stochastic resonance as well, though we have not performed extensive simulations with noise dependence.

In this paper, we introduce a simple phenomenological model for a system of two sheared monolayers to study a novel phase, the melt-freeze phase, first seen in the simulations of Das *et al.* [4, 6]. Using numerical simulations, we observe that the two order parameter model recovers many of the same qualitative features as the simulations from Das *et al.*, especially the dependence on driving force and coupling strength. Our simple model displays new behavior involving the interplay of the order parameters of two adjacent layers. One behavior is that with strong interlayer couplings, two adjacent layers will be in opposite states of matter. Another involves the fluctuation of the order parameters in the melt-freeze phase; fluctuations are larger when both order parameters coexist in the same well than when they are in opposite wells. More simulations on spatially dependent systems are necessary to verify these observations.

Das *et al.* suggested experiments using bulk colloidal crystals, ordered copolymer monolayers, or colloidal monolayers to see this unusual melt-freeze phase [4]. Systems of charged colloidal particles are good candidates

to observe this phenomenon because they possess many properties that are tunable. The review article by Palberg [11] thoroughly discusses the physical properties of charged colloids, how to change the properties, and different measurement techniques. For instance, the interparticle interaction can be adjusted by changing the electrolyte concentration, thereby altering the Coulomb screening. As seen in the simulations, the melt-freeze phenomenon exists only in certain parameter windows, therefore tunable parameters are necessary for experimental observation. The melt-freeze phase and the be-

havior seen in our mean field model could be seen in these experimental systems.

## V. ACKNOWLEDGMENTS

The author acknowledges Moumita Das and Sriram Ramaswamy for informative discussions on their previous simulations. The author also thanks Onuttom Narayan for useful discussions.

- 
- [1] B.N.J. Persson, *Sliding Friction: Physical Principles and Applications, Nanoscience and Technology Series* (Springer, New York, 1998).
  - [2] B.J. Ackerson and N.A. Clark, Phys. Rev. A **30**, 906 (1984).
  - [3] M.J. Stevens and M.O. Robbins, Phys. Rev. E **48**, 3778 (1993).
  - [4] M. Das, G. Ananthakrishna, and S. Ramaswamy, Phys. Rev. E **68**, 061402 (2003).
  - [5] R. Lahiri and S. Ramaswamy, Phys. Rev. Lett. **73**, 1043 (1994).
  - [6] M. Das, S. Ramaswamy, and G. Ananthakrishna, Europhys. Lett. **60**, 636 (2002).
  - [7] B. McNamara and K. Wiesenfeld, Phys. Rev. A **39**, 4854 (1989).
  - [8] Actually, the order parameter cannot represent the structure factor exactly due to its possible negativity, however, the qualitative features are the same.
  - [9] Our strain part of the free energy differs from the one used in [4]. Both forms qualitatively incorporate the characteristics of strain.
  - [10] To be more precise, the signature of stochastic resonance is a peak in the signal-to-noise ratio as a function of noise amplitude.
  - [11] T. Palberg, J. Phys. Condens. Matter **11**, R323 (1999).